

Time-Dependent Channel Formation in a Laser-Produced Plasma

P. E. Young, M. E. Foord, J. H. Hammer, W. L. Kruer, M. Tabak, and S. C. Wilks

University of California, Lawrence Livermore National Laboratory, P.O. Box 5508, Livermore, California 94550

(Received 14 March 1995)

The formation of density channels in an underdense plasma is studied as a function of the laser pulse length. For pulse lengths of less than 300 ps, the channels have a finite axial length and end short of the peak density. As the pulse length is increased beyond 300 ps, the channel lengthens to the opposite side of the density profile and a situation can be obtained in which most of the beam propagates through the plasma within the vacuum propagation cone. The process of channel formation is successfully modeled by two-dimensional hydrodynamic simulations.

PACS numbers: 52.50.Jm, 52.35.Fp, 52.40.Nk, 52.65.Kj

The propagation of an intense laser pulse through a fully ionized plasma is a topic of considerable interest. When the laser intensity is sufficiently large, ponderomotive [1] and thermal [2–4] forces can modify the background plasma distribution leading to whole beam self-focusing and filamentation which can change the propagation of the laser light as well as modify the conditions under which plasma instabilities can grow [5,6]. The propagation of the laser pulse to an intense focus in a plasma has specific applications in inertial confinement fusion (ICF) in the cases of *Hohlraum* entrance holes and the fast ignitor concept [7]. Substantial effort has gone into models of laser beams propagating through large, high density plasmas [8–11], but to date quantitative comparison has been made only to experiments with pulse lengths of 100 ps. Important experimental studies have been made [12] in which a neutral gas was ionized to prepare a channel for a second pulse. When one starts with a high density, full ionized plasma, however, the filamentation instability can interfere with the formation of a density channel. In previous work [13–15] we have shown that a plasma density channel is formed by focused 100 ps laser pulses in the intensity range 1×10^{15} to 5×10^{16} W/cm² and plasma densities greater than $0.1n_c$, where n_c is the critical density at which the electron plasma frequency equals the incident laser frequency. In general, the channel does not go through the plasma but has a finite axial extent due to the onset of the filamentation instability which sprays out the laser light; this requires the threshold is not the fast ignitor ($<0.1n_c$), or the channel is small.

In this Letter, we demonstrate experimentally that the axial extent of the channel is substantially increased and the propagation effects of the plasma are decreased as the pulse length is increased from 100 to 500 ps. This feature is very important for understanding the formation of channels and for successful demonstration of the fast ignitor concept, and shows experimentally the channel behavior on time scales much longer than in previous experiments. This same behavior is observed in two-dimensional LASNEX [16] simulations of the experimental parameters. This behavior occurs because, although the

beam sprays out initially, it still has a high enough intensity to depress the density farther into the plasma, which, over time, leads to the guiding of the beam and enhancement of the channel.

The experiment was conducted using the Janus laser facility at the Lawrence Livermore National Laboratory. The plasma was produced using a 50 J, 2×10^{13} W/cm², 1 ns nominally square laser pulse ($\lambda_0 = 0.532 \mu\text{m}$), which irradiated a $0.5 \mu\text{m}$ thick parylene [(CH)_n] foil. This first pulse burns through the foil and produces an underdense plasma whose peak density decays as a function of time. In this paper, we study the density channels formed by a second pulse of $1.064 \mu\text{m}$ wavelength, which we will call the interaction pulse, which propagates along the same axis as the plasma forming pulse but from the opposite side of the target. The interaction beam [17] is focused with an $f/2$ lens and the best focus is placed, in vacuum, at the target plane. The beam spot at best focus, as measured by an $\sim 2 \mu\text{m}$ resolution imaging system, is radially symmetric and has a $9 \mu\text{m}$ diameter at full width half maximum; because the focal spot is larger than diffraction limited, the beam waist is uniform over a larger distance than one would calculate from the standard Rayleigh range formula. The beam diameter changes by a factor of 2 over a distance of 200 μm on either side of best focus [18]. Models using the measured spot profiles have shown good agreement with the experiment in the past [15].

The background density profile and the density channel were diagnosed using a folded-wave interferometer. The interferometer probe beam had a wavelength of $0.35 \mu\text{m}$ and a pulse width which was varied during the course of the experiment, as will be explained later in this paper.

We monitored the amount of light transmitted through the plasma into an $f/2$ collecting lens. As we demonstrated earlier [15], transmission into this lens is a measure of the filamentation of the interaction beam because low transmission is a consequence of the laser light spraying out to larger angles. After the beam propagates through the plasma and is collected by the $f/2$ lens, the beam is diverted by a dielectric reflector which rejects most of

the $0.53 \mu\text{m}$ backscattered light from the plasma forming beam. All of the light that passes through the $f/2$ lens is collected by a calorimeter that measures the transmitted energy. A 4% reflector before the calorimeter provides light to a fast diode (65 ps rise time) whose signal was recorded on a 4.5 GHz transient digitizer. The diode is filtered with a $1.064 \mu\text{m}$ bandpass filter and samples a small area (0.005 mm^2) of the near field beam pattern (with an area of 78 cm^2) in order to minimize amplitude modulations produced by the interference of rays having different optical paths through the time-dependent plasma distribution.

The experiment consisted of two parts. In the first part, the cavity of the Q -switched, mode-locked oscillator that produced the pulse for both the interferometer probe and the interaction beam was modified to produce Gaussian pulses with FWHM of 100, 250, and 500 ps in order to observe the effect of pulse width on transmission through the plasma. We found that, for sufficiently high energy, the 500 ps pulse produced significantly higher transmission than either the 100 ps pulse or the 250 ps pulse, and we observed, for the first time, a channel that extended into the far side of the plasma. In extensive previous experiments with 100 ps pulses under a variety of laser intensities, focal f numbers, and plasma conditions [18], the channel has never been observed to extend past the peak density. In order to understand the process by which the channel extended itself over longer time periods, in the second part of the experiment the interaction pulse was a nominally square 1 ns pulse, and the relative timing of the interferometer pulse (50 ps FWHM in this case) was varied over many laser pulses in order to investigate the time-dependent development of the laser channel.

The results of the first part of the experiment in which the width of the interaction pulse was varied are summarized in Fig. 1. As we found earlier, with 100 ps pulses at fixed peak density of $0.3n_c$, when the laser beam is below the filamentation threshold (when the laser energy is less than 2 J) all the light is transmitted (excluding a small amount of Brillouin scattered light) within the $f/2$ focusing solid angle. When the filamentation threshold is exceeded, the energy transmitted through the collection optics remains below 20% and is independent of the incident intensity when it is above the filamentation threshold due to the spraying of the light to larger angles as the intensity is increased [15,18]. This behavior is also observed when the pulse is 250 ps FWHM.

When the pulse width is increased to 500 ps, the transmission remains low for moderate intensities. For intensities approaching 10^{16} W/cm^2 , however, the transmission increases substantially, and we observe a channel that extends through the entire plasma (see Fig. 2). Note that because the transmission of the 500 ps pulse at 40 J is the same as that of the shorter pulses, the increase in transmission with the longer pulse at higher energies is due to the pulse length and not due to the decay of the peak density with time. Since the interferometer probe pulse is

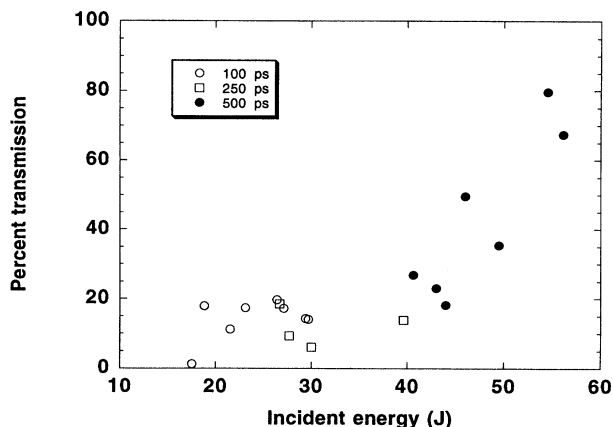


FIG. 1. The percentage of the incident light collected on the transmitted side of the plasma is plotted as a function of incident energy and pulse length. The focusing and collecting lenses are matching $f/2$ optics. The pulse shapes are Gaussian in time.

obtained from the same oscillator as the interaction pulse, for the 500 ps pulse the probe pulse is ~ 250 ps long (due to the frequency conversion process).

For the second part of the experiment, we converted the interaction beam to a 1 ns square pulse and produced a 50 ps interferometer pulse. We could then scan the relative time between the interferometer and the interaction pulses to determine how the channel developed. The result was a series of interferograms which showed the axial propagation of the channel (see Fig. 3). In order to clearly show the evolution of the channel, we have also converted the raw fringe data into the phase distribution produced by the plasma (see Fig. 4). Figure 3(a) shows that at early times, the channel is confined to the incident side of the plasma, while at later times the channel develops and extends to the far side of the plasma [see Figs. 3(b) and 3(c)]. The development of the channel takes place on a time scale of ~ 300 ps, consistent with the results shown in Fig. 1.

The Abel inversions of the interferograms show quantitatively the depth of the channel and the values of the

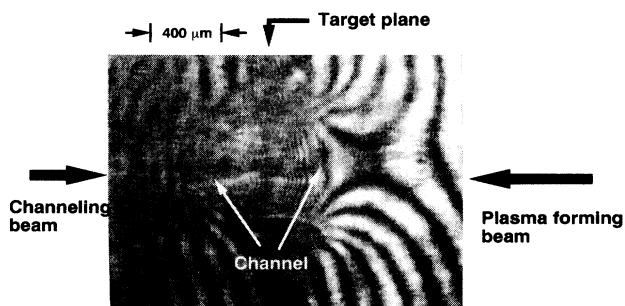


FIG. 2. An interferogram is shown for a case where the incident pulse width is 500 ps and the laser energy is 55 J. A channel of approximate dimensions $800 \mu\text{m}$ long by $100 \mu\text{m}$ wide extends all the way through the plasma.

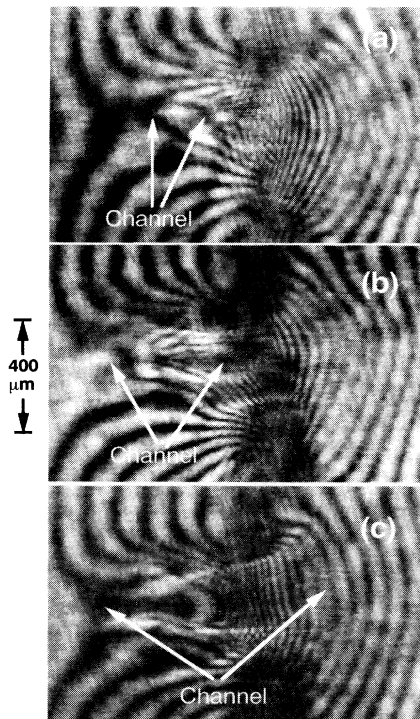


FIG. 3. Interferograms at times relative to the start of the interaction pulse of (a) 50, (b) 195, and (c) 335 ps, showing the evolution of the channel. The arrows point to the ends of the channel. The channel boring beam is a nominally square 1 ns pulse with an energy of (a) 51.5, (b) 53.8, and (c) 48 J.

background density profiles. The depth of the channel in Fig. 4(c) ($t = 335$ ps) reaches 50%, and clearly is the earliest time at which the channel forms on the opposite side of the target. The density profiles also show that the variation of the background density profile is negligible over a 300 ps time scale, which can be seen from the values of the peak density and the spatial extent of the plasma.

The development of the channel is confirmed by the time-dependent measurement of the transmitted light. As seen in Fig. 5, there is an increase in transmission at 300 ps into the pulse which corresponds to the propagation of the density channel to the far side of the plasma. The initial delay between the start of the pulse and the onset of the transmitted light can be decreased by lowering the peak density. By varying the incident laser energy, we also see how the rise time of the transmitted signal is decreased as the energy is increased. The persistence of the diode signal after the end of the incident signal is due to laser light scattered from the target that reflects from objects in the chamber and is delayed ~ 1 ns with respect to the transmitted signal.

Our earlier work [15,18] has established our confidence in the ability to directly compare simulations and experiments. We have used LASNEX simulations to investigate the long time scale channel formation by a 500 ps Gaussian pulse with a Gaussian spatial profile that has a

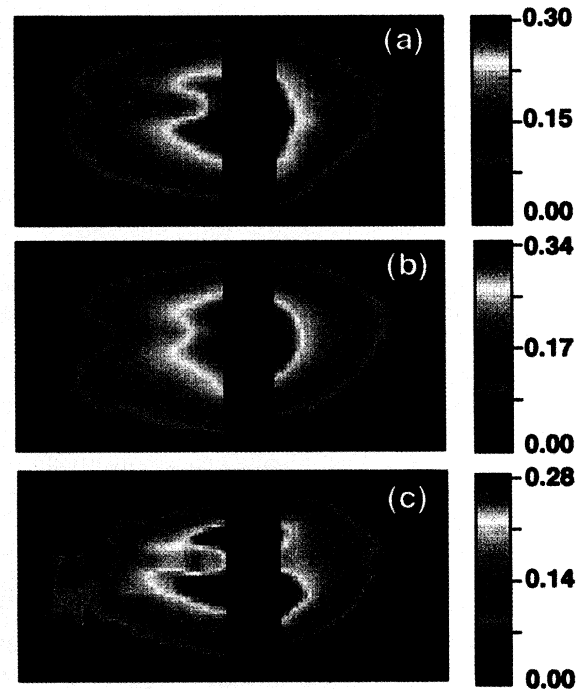


FIG. 4(color). Density profiles obtained by Abel inverting the interferograms of Fig. 3. The color levels are relative density, n_e/n_c . The areas of the figures equal those shown in Fig. 3.

FWHM = $13 \mu\text{m}$ (transverse, $I_{\text{max}} = 5 \times 10^{15} \text{ W/cm}^2$, $n_{e,\text{max}} = 0.2n_c$, $T_e = 1 \text{ keV}$, $T_i = 500 \text{ eV}$). We include temperature effects with a modified inverse bremsstrahlung absorption, with a flux limit of 0.03. In Fig. 6, we have plotted the density distributions at three different times showing that the evolution of the channel is very similar to that observed experimentally. In this figure, the channel forming beam is incident from the left side of the picture and propagates into a parabolic density profile whose peak

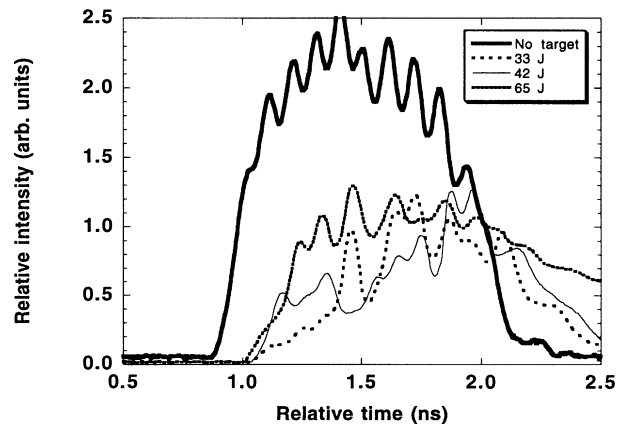


FIG. 5. Transmitted diode signals with and without a plasma. As the interaction beam energy increases, the transmitted signal rises at a more rapid rate. The measured transmission by the calorimeter is 50% when the incident energy is 65 J.

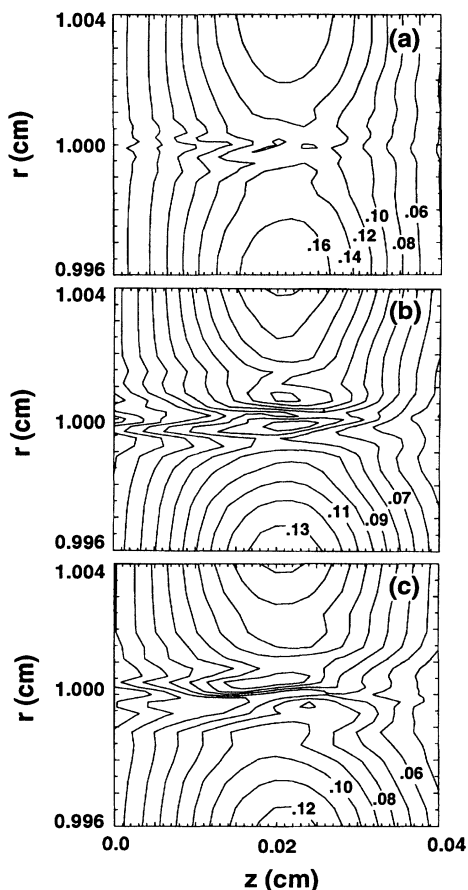


FIG. 6. Results from LASNEX simulations showing the time evolution of the density channel. Shown are density contours at (a) $t = 300$ ps, (b) $t = 450$ ps, and (c) $t = 500$ ps, where the peak of the Gaussian laser pulse is at $t = 500$ ps. The peak of the background density profile is initially at $z = 0.02$ cm.

is at $z = 0.02$ cm. At an early time, the channel is confined to the left side of the peak of the density profile due to the onset of the filamentation instability. At later times, the beam extends to the opposite side of the target on a time scale of about 250 ps, with a density perturbation of about 50%, in agreement with experiment.

To obtain a scaling for the channel formation time, we consider the ejection of ions by the ponderomotive force. If we assume that the ponderomotive pressure is much greater than the plasma pressure and take the radial intensity distribution to be $I_0 \exp[-(1/2)(r/r_0)^2]$, the equation of motion becomes

$$\ddot{\xi} = \xi e^{-\xi^2/2}. \quad (1)$$

Here $\xi = r/r_0$, time is normalized in units of $\tau_0 = r_0/\sqrt{(Zm/4M)v_{os}^2}$, and v_{os} is the electron oscillatory velocity at $r = 0$. A typical time for an ion to be expelled (for example, to move from $\xi = 0.5$ to $\xi = 3$) is about $(3-4)\tau_0$. For the example considered in this paper, the ejection time is about 100 ps for peak intensity. The finite rise time of the pulse and the finite plasma pressure

will both increase this time. The time is also increased because of the lower intensity produced by the spraying of the light by the filamentation instability.

The experiments also show that the time scale for the formation of the channel and the amount of transmitted light within the focusing solid angle depends on the pulse shape. The percentage transmission of the square pulse was 50% compared to 80% for the 500 ps Gaussian. It is plausible that a pulse that turns on adiabatically will have better propagation characteristics than one that turns on rapidly; i.e., it has a rise time that is shorter than the channel formation time.

In summary, we have demonstrated that the laser pulse length is a very important parameter for propagating a laser beam through a relatively high density plasma, a result which is a necessary condition for the success of the fast ignitor concept. We have shown that the laser beam initially spreads due to filamentation, but is still of sufficient intensity to depress the plasma density and initiate a self-guiding process that, if the pulse is long enough, leads to the formation of a coherent channel.

We acknowledge useful discussions with J. Woodworth. We would like to thank W. Cowens, R. Gonzales, and G. London for operating the Janus laser during the experiment, and D. Chakedis, A. Ellis, and R. Robinson for producing targets. This work was performed under the auspices of the U.S. Department of Energy by the Lawrence Livermore National Laboratory under Contract No. W-7405-Eng-48.

- [1] P. K. Kaw *et al.*, Phys. Fluids **16**, 1522 (1973).
- [2] V. K. Tripathi and L. A. Pitale, Appl. Phys. **48**, 3288 (1977).
- [3] R. S. Craxton and R. L. McCrory, J. Appl. Phys. **56**, 108 (1984).
- [4] K. Estabrook *et al.*, Phys. Fluids **28**, 19 (1985).
- [5] C. S. Liu and V. K. Tripathi, Phys. Fluids **29**, 4188 (1986).
- [6] H. C. Barr *et al.*, Phys. Rev. Lett. **56**, 2256 (1986); Phys. Fluids **31**, 641 (1988).
- [7] M. Tabak *et al.*, Phys. Plasma **1**, 1626 (1994).
- [8] R. H. Lehmburg *et al.*, J. Appl. Phys. **62**, 2680 (1987); A. J. Schmitt, Phys. Fluids B **3**, 186 (1991).
- [9] E. Epperlein, Phys. Rev. Lett. **65**, 2145 (1990); E. Epperlein and R. W. Short, Phys. Fluids B **4**, 2211 (1992).
- [10] R. L. Berger *et al.*, Phys. Fluids B **5**, 2243 (1993).
- [11] M. R. Amin *et al.*, Phys. Fluids B **5**, 3748 (1993); V. V. Eliseev *et al.*, Phys. Plasma (to be published).
- [12] C. G. Durfee III and H. M. Milchberg, Phys. Rev. Lett. **71**, 2409 (1993).
- [13] P. E. Young *et al.*, Phys. Rev. Lett. **63**, 2812 (1989).
- [14] P. E. Young, Phys. Fluids B **3**, 2331 (1991).
- [15] S. C. Wilks *et al.*, Phys. Rev. Lett. **73**, 2994 (1994).
- [16] G. D. Zimmerman and W. L. Kruer, Comments Plasma Phys. Controlled Fusion **2**, 51 (1977).
- [17] P. E. Young and K. G. Estabrook, Phys. Rev. E **49**, 5556 (1994).
- [18] P. E. Young *et al.*, Phys. Plasma **2**, 7 (1995).

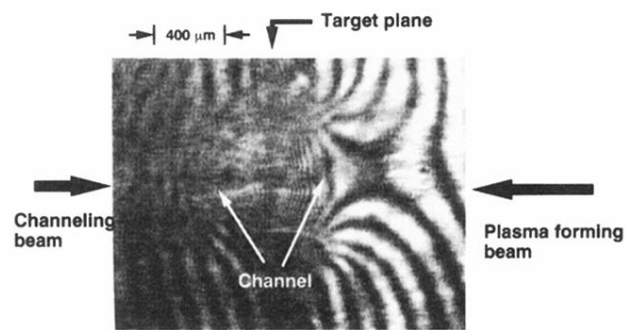


FIG. 2. An interferogram is shown for a case where the incident pulse width is 500 ps and the laser energy is 55 J. A channel of approximate dimensions 800 μm long by 100 μm wide extends all the way through the plasma.

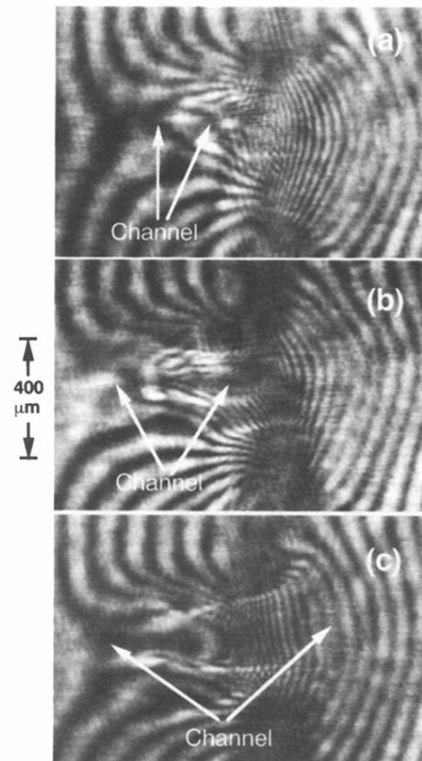


FIG. 3. Interferograms at times relative to the start of the interaction pulse of (a) 50, (b) 195, and (c) 335 ps, showing the evolution of the channel. The arrows point to the ends of the channel. The channel boring beam is a nominally square 1 ns pulse with an energy of (a) 51.5, (b) 53.8, and (c) 48 J.

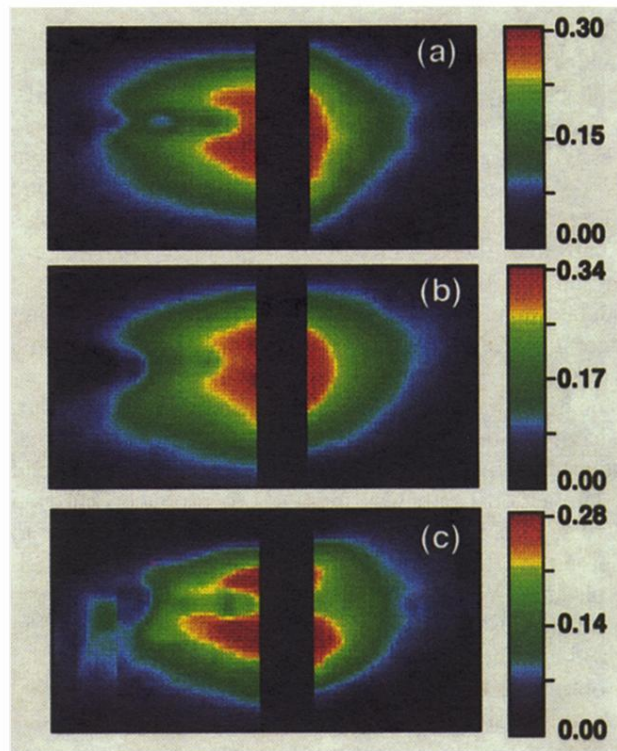


FIG. 4(color). Density profiles obtained by Abel inverting the interferograms of Fig. 3. The color levels are relative density, n_e/n_c . The areas of the figures equal those shown in Fig. 3.